Generation of Ince–Gaussian beams in highly efficient, nanosecond Cr, Nd:YAG microchip lasers

2013 Laser Phys. Lett. 10 085803

(http://iopscience.iop.org/1612-202X/10/8/085803)

IOP PUBLISHING LASER PHYSICS LETTERS
Laser Phys. Lett. **10** (2013) 085803 (7pp) doi:10.1088/1612-2011/10/8/085803

LETTER

Generation of Ince–Gaussian beams in highly efficient, nanosecond Cr, Nd:YAG microchip lasers

J Dong[1], J Ma[1], Y Y Ren[1], G Z Xu[1] and A A Kaminskii[2]

[1] Department of Electronics Engineering, School of Information Science and Technology, Xiamen University, Xiamen 361005, People's Republic of China
[2] Institute of Crystallography, Russian Academy of Sciences, Leninsky Prospekt 59, Moscow 119333, Russia

E-mail: jdong@xmu.edu.cn and kaminalex@mail.ru

Received 2 August 2012, in final form 19 September 2012
Accepted for publication 21 September 2012
Published 14 June 2013
Online at stacks.iop.org/LPL/10/085803

Abstract
Direct generation of higher-order Ince–Gaussian (IG) beams from laser-diode end-pumped Cr, Nd:YAG self-*Q*-switched microchip lasers was achieved with high efficiency and high repetition rate. An average output power of over 2 W was obtained at an absorbed pump power of 8.2 W; a corresponding optical-to-optical efficiency of 25% was achieved. Various IG modes with nanosecond pulse width and peak power of over 2 kW were obtained in laser-diode pumped Cr, Nd:YAG microchip lasers under different pump power levels by applying a tilted, large area pump beam. The effect of the inversion population distribution induced by the tilted pump beam and nonlinear absorption of Cr^{4+}-ions for different pump power levels on the oscillation of higher-order IG modes in Cr, Nd:YAG microchip lasers is addressed. The higher-order IG mode oscillation has a great influence on the laser performance of Cr, Nd:YAG microchip lasers.

(Some figures may appear in colour only in the online journal)

1. Introduction

In addition to the Laguerre–Gaussian and Hermite–Gaussian beams generated in stable laser resonators which are used for different transverse laser field distributions, Ince–Gaussian (IG) beams have been proposed recently and have gained a great deal of attention due to their various transverse distributions and their flexibility. IG beams generated in stable laser resonators are not only a third complete family of the paraxial-wave equation in elliptic cylindrical coordinates, but they also constitute the continuous transition modes between Hermite–Gaussian and Laguerre–Gaussian modes when their ellipticity is chosen appropriately [1, 2]. Ince–Gaussian beams have been demonstrated for manipulation of microparticles [3], formation of various optical vortices for optical trapping and optical tweezers [4]. IG beams have been generated in laser-diode pumped solid-state Nd:YVO_4 lasers by breaking the symmetry of the resonator by shifting the output coupler sideways several tens of micrometers or introducing an additional cross hair [5]. Forced IG mode operations were achieved in $LiNdP_4O_{12}$ and Nd:$GdVO_4$ miniature lasers by tilting the central axis of the resonator with respect to the axis of the laser-diode pump beam [6]. However, the output power from these solid-state lasers is low and the lasers are less efficient. Cr, Nd:YAG crystal is an excellent self-*Q*-switched laser material and is formed by co-doping Cr ions and Nd ions into YAG crystal by adding extra Ca^{2+}-ions as charge compensators.

Laser-diode pumped self-Q-switched Cr, Nd:YAG monolithic miniature lasers have been demonstrated with nanosecond and picosecond pulse width [7, 8]. Complicated transverse patterns have been generated in Cr, Nd:YAG microchip lasers by adjusting the pump beam diameter inside the Cr, Nd:YAG crystal [9]. The high gain of Nd^{3+} ions together with the nonlinear absorption of Cr^{4+} ions in Cr, Nd:YAG crystal makes generation of nanosecond pulse width, high peak power higher-order IG modes possible by applying a tilted, large area pump beam from a laser-diode. Compact, highly efficient, nanosecond pulse width and over kW peak power Cr, Nd:YAG higher-order IG mode microchip lasers may have potential applications in manipulation of microparticles and formation of optical solitons and optical vertices.

In this letter, we report direct generation of Ince–Gaussian beams from highly efficient, nanosecond pulse-width laser-diode end-pumped Cr, Nd:YAG self-Q-switched microchip lasers by adjusting the azimuthal symmetry of the pump beam incident on the Cr, Nd:YAG crystal. An optical-to-optical efficiency of 25% has been obtained. Various high-order IG beams were generated under different pump power levels. The obtained higher-order IG modes from the Cr, Nd:YAG microchip lasers were determined from the corresponding patterns calculated analytically using IG mode expressions by adjusting the ellipticity. The saturated inversion population distribution induced by the tilted pump beam and the nonlinear absorption of Cr^{4+}-ions in Cr, Nd:YAG crystal play important roles in the generation of higher-order IG beams in Cr, Nd:YAG microchip lasers. The effect of higher-order mode oscillation on the average output power of Cr, Nd:YAG microchip lasers is also addressed.

2. Experimental setup

Figure 1 shows a schematic diagram of the experimental setup for generation of IG beams from a laser-diode end-pumped Cr, Nd:YAG self-Q-switched microchip laser. A plane–parallel 1.8 mm-thick Cr, Nd:YAG crystal doped with 1 at.% Nd and 0.01 at.% Cr was used as the gain medium for generating self-Q-switched laser pulses. One surface of the Cr, Nd:YAG crystal was coated for antireflection at 808 nm and high reflection at 1064 nm to act as the rear mirror of the laser cavity; the other surface was coated for antireflection at 1064 nm to reduce the intracavity loss and high reflection at 808 nm to increase the absorption efficiency of the pump power. A plane–parallel BK7 output coupler with reflection (R_{OC}) of 90% at 1064 nm was mechanically attached to the Cr, Nd:YAG crystal tightly. The total cavity length was 1.9 mm by considering the coating thickness on both sides of the Cr, Nd:YAG crystal. A high power fiber coupled 808 nm laser-diode with a core diameter of 400 μm and numerical aperture of 2.2 was used as the pump source. An optical coupling system with two lenses with focal lengths of $f_1 = 8$ mm and $f_2 = 15$ mm was used to collimate and focus the pump beam on the rear surface of the Cr, Nd:YAG crystal. A pump beam diameter of 200 μm was incident on the Cr, Nd:YAG self-Q-switched crystal after the optical collimating and focusing system. The Cr, Nd:YAG crystal

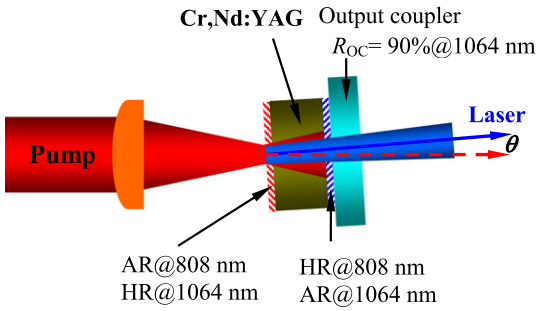

Figure 1. Schematic diagram of the laser-diode pumped Cr, Nd:YAG self-Q-switched microchip laser for generation of IG beams.

was tilted several degrees away from the incident pump beam for generation of IG higher-order modes, as shown in figure 1. The output laser characteristics were recorded with an InGaAs photodiode and a 400 MHz oscilloscope. The laser emitting spectra were monitored with an Ando optical spectral analyzer. The beam profile was monitored and recorded with a Thorlabs BC106-VIS CCD beam profiler.

3. Results and discussion

Because Nd^{3+}-ions in YAG comprise a four-level laser system with a large emission cross section, the laser threshold is easier to reach for higher-order transverse modes in laser-diode pumped Cr, Nd:YAG self-Q-switched microchip lasers. A plane–parallel Fabry–Perot cavity was used in the experiments; the laser emitting area still matched the laser pump beam well even with the pump beam from the laser-diode tilting away from the laser propagation direction of the Cr, Nd:YAG microchip laser. Nonlinear absorption of Cr^{4+}-ions along the laser's propagation and radial directions has a great effect on the inversion population distribution in Cr, Nd:YAG crystal. When longitudinally pumped by a large area, tilted Gaussian beam from a laser-diode, the inversion population distribution in Cr, Nd:YAG crystal forces plane–parallel microchip lasers to oscillate in IG modes. Higher-order IG modes were excited at high pump power level when the pump beam diameter was kept constant in the laser experiments. The IG mode oscillation in laser-diode pumped Cr, Nd:YAG microchip lasers can be chosen by adjusting the tilting angle of the incident pump beam on the Cr, Nd:YAG crystal. Figure 2 shows some typical IG mode transverse field distributions observed experimentally under different pump power levels when the incident pump beam was 5° away from the laser propagation direction of the Cr, Nd:YAG microchip laser. A stable $IG^{e}_{2,2}$ mode was observed at an absorbed pump power of 1.3 W, as shown in figure 2(a). The mode number increases with the absorbed pump power. Various stable higher-order IG modes such as $IG^{o}_{6,2}$, $IG^{e}_{4,4}$, $IG^{o}_{5,3}$, $IG^{e}_{10,4}$, $IG^{e}_{10,8}$, $IG^{e}_{12,8}$ modes were obtained at different pump power levels when the absorbed pump power was kept below 5.5 W, as shown in figures 2(b)–(g). More complicated transverse laser field distributions were observed at different pump

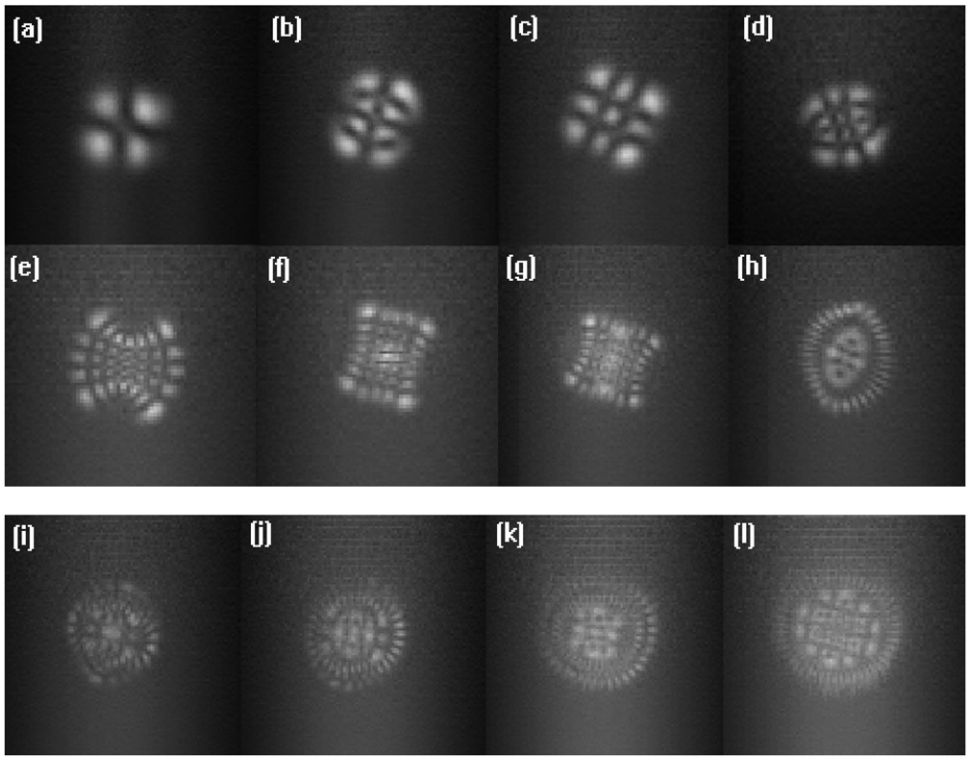

Figure 2. Various IG beam transverse intensity distributions observed in laser-diode pumped Cr, Nd:YAG self-Q-switched lasers under different pump power levels. (a) $P_{\rm abs} = 1.3$ W, (b) $P_{\rm abs} = 1.7$ W, (c) $P_{\rm abs} = 2.2$ W, (d) $P_{\rm abs} = 3.5$ W, (e) $P_{\rm abs} = 3.9$ W, (f) $P_{\rm abs} = 4.3$ W, (g) $P_{\rm abs} = 4.8$ W, (h) $P_{\rm abs} = 5.6$ W, (i) $P_{\rm abs} = 6.5$ W, (j) $P_{\rm abs} = 7.3$ W, (k) $P_{\rm abs} = 7.8$ W, (l) $P_{\rm abs} = 8.2$ W.

power levels when the absorbed pump power was higher than 5.5 W owing to two or three sets of IG modes oscillating simultaneously. Figures 2(h)–(k) show $\mathrm{IG}^{\rm e}_{4,4} + \mathrm{IG}^{\rm e}_{16,16}$, $\mathrm{IG}^{\rm e}_{14,12} + \mathrm{IG}^{\rm o}_{5,3}$, $\mathrm{IG}^{\rm e}_{17,15} + \mathrm{IG}^{\rm o}_{7,3}$, $\mathrm{IG}^{\rm o}_{21,19} + \mathrm{IG}^{\rm e}_{7,5}$, i.e. two IG modes oscillating simultaneously at different pump power levels. Figure 2(l) shows $\mathrm{IG}^{\rm o}_{25,25} + \mathrm{IG}^{\rm e}_{5,5} + \mathrm{IG}^{\rm e}_{8,4}$, i.e. three IG modes oscillating simultaneously at an absorbed pump power of 8.2 W. All the laser beams generated in the Cr, Nd:YAG microchip lasers exhibit symmetric transverse distributions even with higher-order IG mode oscillation or complicated mixed mode oscillation.

The mode numbers and ellipticities of the different IG modes generated in the Cr, Nd:YAG microchip lasers were determined from correspondence to patterns calculated analytically using the IG mode expressions. The transverse field distribution of IG modes in any plane along the laser propagation direction, z, can be expressed in terms of even (C^m_p) and odd (S^m_p) Ince polynomials of order p and degree m, and ellipticity parameter ε [2, 1],

$$\mathrm{IG}^{\rm e}_{p,m}(r,\varepsilon) = \frac{Aw_0}{w(z)} C^m_p(\mathrm{i}\xi,\varepsilon) C^m_p(\eta,\varepsilon) \exp\left[\frac{-r^2}{w^2(z)}\right] \times \exp\left[kz + \frac{kr^2}{2R(z)} - (p+1)\psi_z(z)\right] \quad (1)$$

$$\mathrm{IG}^{\rm o}_{p,m}(r,\varepsilon) = \frac{Bw_0}{w(z)} S^m_p(\mathrm{i}\xi,\varepsilon) S^m_p(\eta,\varepsilon) \exp\left[\frac{-r^2}{w^2(z)}\right] \times \exp\left[kz + \frac{kr^2}{2R(z)} - (p+1)\psi_z(z)\right] \quad (2)$$

with normalized constant A, B, laser beam width $w(z)$, laser beam waist w_0 at $z = 0$; the superscripts e and o refer to even and odd modes, respectively. The elliptic coordinates were defined as $x = f(z)\cosh(\xi)\cos(\eta)$, $y = f(z)\sinh(\xi)\sin(\eta)$, and $z = z$, where $f(z) = f_0 w(z)/w_0, f_0$ is the semifocal separation at the waist plane $z = 0$, and ξ, η are the radial and angular elliptic variables, respectively. r is the radial direction in the plane transverse to the laser propagation direction, $R(z) = z + z^2_{\rm R}/z$ is the radius of curvature of the phase front, $\psi_z(z) = \arctan(z/z_{\rm R})$ is the Gouy shift, $z_{\rm R} = kw^2_0/2$ is the Rayleigh length, k is the wavenumber.

The theoretical prediction of IG mode oscillation in laser-diode pumped Cr, Nd:YAG self-Q-switched lasers was made by applying equations (1) and (2). The mode number $[p, m]$ and the ellipticity parameter ε of different IG transverse modes observed in laser-diode pumped Cr, Nd:YAG self-Q-switched microchip lasers are determined by corresponding numerical calculations of laser transverse distribution, as shown in figure 3. The theoretical calculated transverse patterns of IG modes, as shown in figures 3(a)–(g), and superposition of two IG modes oscillating simultaneously, as shown in figure 3(h), are in good agreement with the transverse patterns observed in experiments (as shown in figures 2(a)–(h)) and further confirm that the laser oscillated at different even and odd IG modes.

The IG mode oscillation of the laser-diode pumped microchip Cr, Nd:YAG self-Q-switched laser was governed by the initial inversion population of the Cr, Nd:YAG laser, the inversion population distribution provided by the pump beam

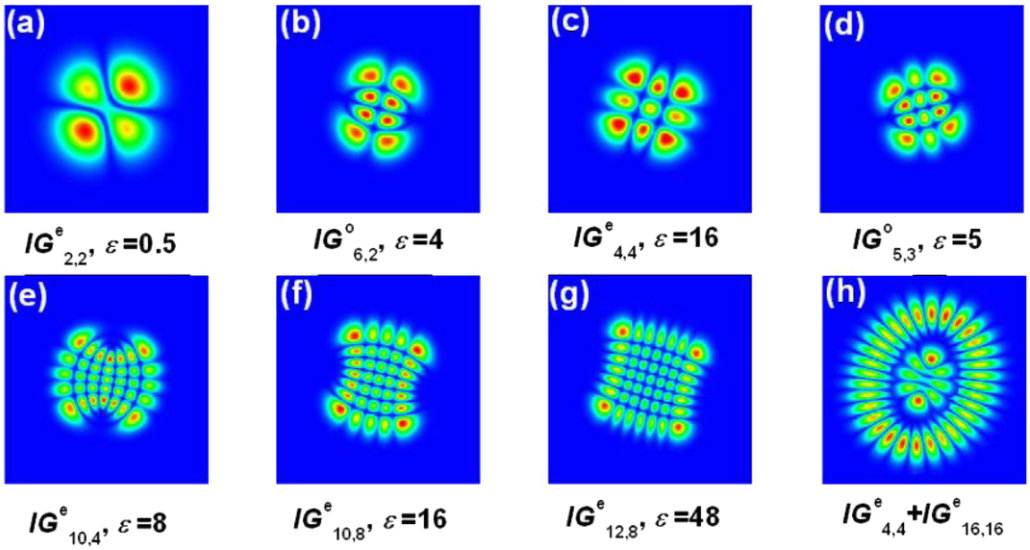

Figure 3. Analytical reconstruction of some typical IG modes observed in laser-diode pumped Cr, Nd:YAG self-Q-switched microchip lasers.

and the nonlinear absorption of Cr^{4+} ions in Cr, Nd:YAG crystal under high intracavity laser intensity. The initial inversion population of the Cr, Nd:YAG self-Q-switched laser under continuous-wave pumping can be expressed as

$$N_{\mathrm{i}} = [2\sigma_{\mathrm{g}} N_{\mathrm{s0}} l + \ln(1/R_{\mathrm{OC}}) + \delta_{\mathrm{Loss}}]/(2\sigma l) \tag{3}$$

where σ and σ_{g} are the emission cross sections of Cr, Nd:YAG crystal and the ground-state absorption cross section of Cr^{4+}:YAG saturable absorber, N_{s0} is the total concentration of Cr^{4+} in the YAG, l is the length of the Cr, Nd:YAG crystal, R_{OC} is the reflectivity of the output coupler, and δ_{Loss} is the total intracavity loss.

When the pump spot is been assumed to be circular and the intensity distribution is assumed to be a Gaussian profile, for a thin gain medium longitudinally pumped by the continuous-wave incident pump power P_{in} in a two-pass pumping configuration, the saturated inversion population under high laser intensity can be expressed as follows:

$$N_{\mathrm{sat}}(r, z) = \Delta N(r, z)/[1 + I(r, z)/I_{\mathrm{sat}}] \tag{4}$$

where $I(r, z)$ is the intensity of the laser mode inside the cavity and I_{sat} is the laser saturation intensity of the gain medium. $\Delta N(r, z)$ is the spatial distribution of the population inversion provided by pump beam, and is expressed as

$$\Delta N(r, z) = \frac{2P_{\mathrm{in}}\alpha f_{\mathrm{a}}\tau}{h\nu_{\mathrm{p}}\pi w_{\mathrm{p}}^2(z)} \exp\left(\frac{-2r^2}{w_{\mathrm{p}}^2(z)}\right) \times [\exp(-\alpha z) + \exp(-\alpha(2l - z))] \tag{5}$$

where r is the radial direction in the plane transverse to the laser propagation direction, z is the laser propagation direction, h is the Planck constant, ν_{p} is the frequency of the pump power, τ is the fluorescence lifetime of the gain medium, α is the absorption coefficient of the gain medium at pump wavelength λ_{p}, l is the length of the Cr, Nd:YAG crystal, f_{a} is the fractional equilibrium Boltzmann population of the upper laser level in the crystal field component (1 for a four-level system), and $w_{\mathrm{p}}(z)$ is the pump beam waist at pump beam position z.

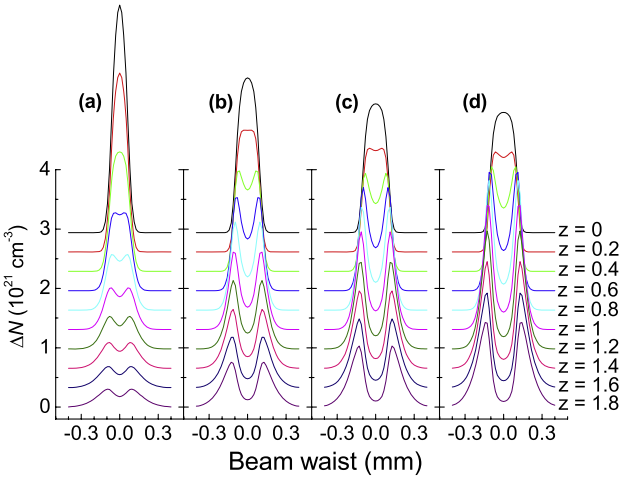

Figure 4. Variation of saturated inversion populations inside Cr, Nd:YAG crystal with beam waist under different pump power levels: (a) $P_{\mathrm{abs}} = 1.3$ W, (b) $P_{\mathrm{abs}} = 3.9$ W, (c) $P_{\mathrm{abs}} = 5.6$ W, (d) $P_{\mathrm{abs}} = 8.2$ W.

The radial saturated inversion population distribution at different positions z inside a 1.8 mm-thick Cr, Nd:YAG crystal under different pump power levels when the pump beam is normally incident on the Cr, Nd:YAG crystal is shown in figure 4. The saturated inversion population decreases with z in Cr, Nd:YAG crystal for different pump powers. The saturated inversion population inside Cr, Nd:YAG crystal has a characteristic local minimum on the light axis when z is larger than 0.4 mm; the inversion population along the light axis decreases and the inversion population away from the light axis increases with pump power. The inversion population distribution tends to be broadened. The saturated inversion population distribution inside the Cr, Nd:YAG crystal under high pump power intensity forms the gain

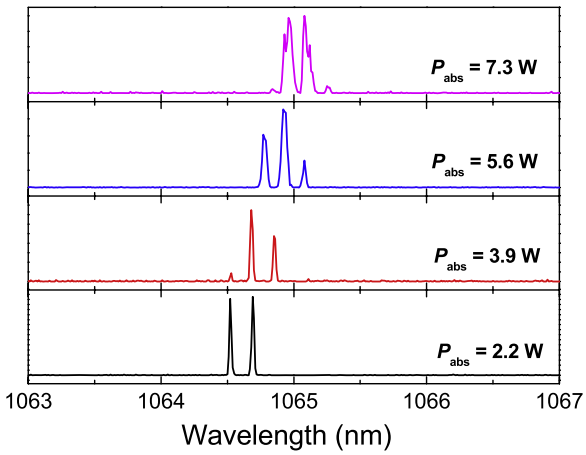

Figure 5. Laser spectra of Cr, Nd:YAG self-*Q*-switched lasers under different pump power levels.

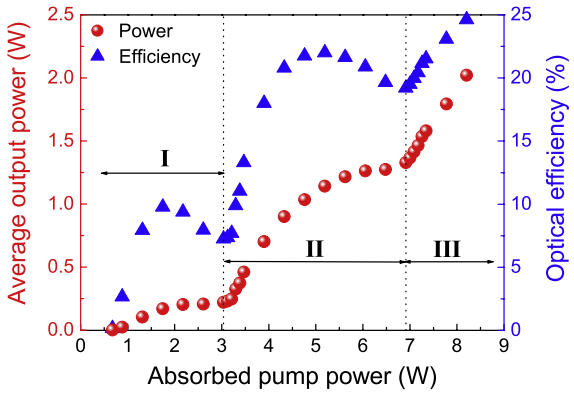

Figure 6. Average output power and optical-to-optical efficiency of a Cr, Nd:YAG self-*Q*-switched microchip laser as a function of the absorbed pump power.

guiding for transverse mode oscillation. The multi-transverse IG modes compete for inversion population distribution along the radial and light directions in Cr, Nd:YAG crystal; two sets or three sets of IG modes oscillate simultaneously owing to the broadened inversion population distribution at high pump power.

The formation of high-order IG modes in a laser-diode end-pumped Cr, Nd:YAG microchip laser is attributed to the tilted large area pump beam incident on the Cr, Nd:YAG crystal and the nonlinear absorption of the Cr^{4+} ion saturable absorber. For the Cr, Nd:YAG self-*Q*-switched laser crystal used in the experiments, the concentration of Nd^{3+} ions is about 1.38×10^{20} cm^{-3} and the concentration of Cr^{4+} ions is about 4.65×10^{16} cm^{-3}; therefore, the ratio of Nd^{3+} ions to Cr^{4+} ions is about 3000. It is reasonable to assume that the Nd^{3+} ions and Cr^{4+} ions are homogeneously distributed in the Cr, Nd:YAG crystal. The intracavity laser intensity enhanced by nonlinear absorption of Cr^{4+} ions has a great effect on the saturated inversion population distribution inside the Cr, Nd:YAG crystal and forms gain guiding for higher-order mode oscillation. Therefore, the higher-order IG modes were forced to oscillate in the Cr, Nd:YAG microchip lasers.

Although the emission bandwidth of Nd^{3+} ions in Cr, Nd:YAG is very narrow (about 1 nm [10]), the Cr, Nd:YAG microchip lasers oscillated in multi-longitudinal modes owing to the 1.8 mm-thick Cr, Nd:YAG used in the experiments. The laser emitting spectra of laser-diode pumped Cr, Nd:YAG microchip lasers at different pump power levels are shown in figure 5. The lasers oscillated in two longitudinal modes when the absorbed pump power was lower than 2.3 W. Then the lasers oscillated in three longitudinal modes with further increase of the pump power until the absorbed pump power reached 7.2 W. The lasers oscillated in four longitudinal modes with further increase of pump power. The separation of longitudinal modes of a laser-diode pumped Cr, Nd:YAG microchip laser is estimated to be 0.16 nm, which is in good agreement with the free spectral range between the resonant modes (0.163 nm) in the laser cavity filled with gain medium predicted by [11] $\Delta\lambda_c = \lambda^2/2L_c$, where L_c is the optical length of the resonator and λ is the laser wavelength. The laser emitting wavelength shifts to longer wavelength with absorbed pump power owing to the emission spectrum change with temperature [12, 13] due to the heat generated in Cr, Nd:YAG crystal under high pump power levels.

Multi-longitudinal mode oscillation in Cr, Nd:YAG microchip lasers has some influence on the average output power, and the evolution of higher-order IG mode oscillation with pump power in Cr, Nd:YAG microchip lasers has a great effect on the laser performance. The average output power and optical-to-optical efficiency of a laser-diode pumped Cr, Nd:YAG self-*Q*-switched microchip laser as a function of absorbed pump power are shown in figure 6. The absorbed pump power threshold for lasing is about 0.68 W. The average output power does not increase linearly with absorbed pump power in the whole available pump power region. There are three regions for variation of average output power with the absorbed pump power. The average output power increases linearly with the absorbed pump power when the absorbed pump power is higher than the absorbed pump power threshold. However, the average output power tends to saturate when the absorbed pump power is higher than 2 W. This is caused by the variation of IG modes under different absorbed pump power levels. The mode number of the IG mode increases with absorbed pump power, and IG modes compete with each other for the inversion population provided by the pump power. Therefore, higher-order IG mode oscillation competing for the inversion population makes the average output power increase slowly with absorbed pump power. When the higher-order IG modes fully oscillate simultaneously, the average output power increases linearly again in region II in figure 6 when the absorbed pump power is higher than 3.1 W and the slope efficiency is about 65% with respect to the absorbed pump power. The average output power increases slowly with absorbed pump power when the absorbed pump power is higher than 4.5 W and tends to be saturated until an absorbed pump power of 6.9 W. This is caused by the second IG mode oscillating and competition for the inversion population provided by the pump power. Therefore, two or three IG modes competing with each other

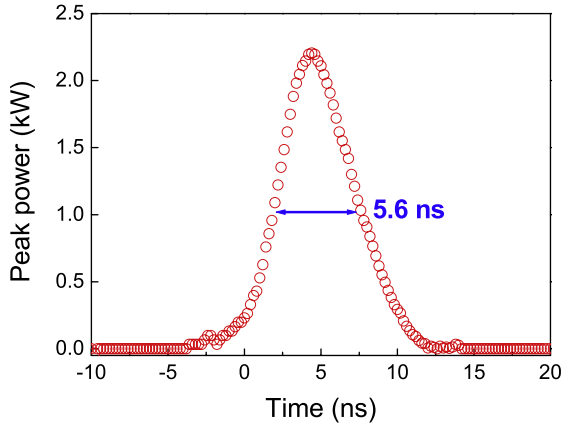

Figure 7. The nanosecond pulse-width, peak power of over 2.2 kW laser pulse obtained for a Cr, Nd:YAG self-Q-switched laser; the repetition rate is 73.3 kHz.

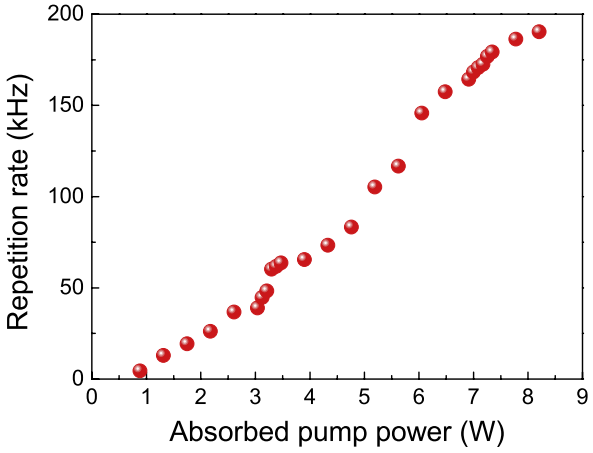

Figure 8. Repetition rate of Cr, Nd:YAG self-Q-switched lasers as a function of the absorbed pump power.

for the inversion population around the threshold of second or third IG mode oscillation is the cause of the slow increase of average output power with absorbed pump power. When the absorbed pump power is higher than 6.9 W, the second or third IG modes fully oscillate and fully extract the energy stored in the Cr, Nd:YAG crystal together with the main IG mode. Therefore, the average output power increases linearly with the absorbed pump power (as shown in region III in figure 6) and the slope efficiency is over 55%. A maximum average output power of over 2 W was obtained when the absorbed pump power was 8.2 W; the corresponding optical-to-optical efficiency was about 25% with respect to the absorbed pump power. The corresponding optical-to-optical efficiency as a function of the absorbed pump power is also given in figure 6. The nonlinear variation of the average output power with the absorbed pump power of Cr, Nd:YAG self-Q-switched microchip lasers is attributed to the higher-order IG mode oscillation.

Figure 7 shows a typical oscilloscope pulse profile of a Cr, Nd:YAG self-Q-switched microchip laser when the absorbed pump power is 4.3 W. A laser pulse with a pulse energy of 12.4 μJ and a pulse width (FWHM) of 5.6 ns was obtained under an absorbed pump power of 4.3 W. The corresponding peak power of the Cr, Nd:YAG self-Q-switched microchip laser was over 2.2 kW. The laser worked at 73.3 kHz. The repetition rate of laser-diode pumped Cr, Nd:YAG microchip lasers increases nearly linearly with absorbed pump power, as shown in figure 8. The repetition rate increases from several kHz just above the absorbed pump power threshold up to 190 kHz when an absorbed pump power of 8.2 W is applied.

4. Conclusions

Highly efficient, nanosecond pulse-width Ince–Gaussian mode oscillation was achieved in laser-diode pumped Cr, Nd:YAG self-Q-switched microchip lasers by tilting the pump beam incident on the Cr, Nd:YAG crystal. Various IG beams with nanosecond pulse width and over kW peak power were obtained by adjusting the pump power levels. A single IG beam was obtained when the absorbed pump power was lower than 5.5 W and complicated IG beams combining two or three IG modes were observed when the absorbed pump power was higher than 5.5 W. An average output power of over 2 W was obtained at an absorbed pump power of 8.2 W; a corresponding optical-to-optical efficiency of 25% was achieved. The laser oscillated at a high repetition rate depending on the pump power level; 190 kHz repetition rate has been achieved in laser-diode pumped Cr, Nd:YAG microchip lasers.

Acknowledgments

This work was supported by the Program for New Century Excellent Talents in University (NCET) under Grant No. NCET-09-0669, the Fundamental Research Funds for the Central Universities (No. 2010121058), and the PhD Programs Foundation of the Ministry of Education of China (No. 20100121120019). A A Kaminskii is grateful for partial support from the Russian Foundation for Basic Research and the Program of the Presidium of Russian Academy of Sciences 'Extreme laser fields and their applications'.

References

[1] Bandres M A and Gutierrez-Vega J C 2004 Ince–Gaussian beams *Opt. Lett.* **29** 144–6
[2] Bandres M A and Gutierrez-Vega J C 2004 Ince–Gaussian modes of the paraxial wave equation and stable resonators *J. Opt. Soc. Am.* A **21** 873–80
[3] Woerdemann M, Alpmann C and Denz C 2011 Optical assembly of microparticles into highly ordered structures using Ince–Gaussian beams *Appl. Phys. Lett.* **98** 111101
[4] Chu S C, Yang C S and Otsuka K 2008 Vortex array laser beam generation from a Dove prism-embedded unbalanced Mach–Zehnder interferometer *Opt. Express* **16** 19934–49
[5] Schwarz U T, Bandres M A and Gutierrez-Vega J C 2004 Observation of Ince–Gaussian modes in stable resonators *Opt. Lett.* **29** 1870–2

[6] Ohtomo T, Kamikariya K, Otsuka K and Chu S C 2007 Single-frequency Ince–Gaussian mode operations of laser-diode-pumped microchip solid-state lasers *Opt. Express* **15** 10705–17
[7] Dong J, Deng P, Lu Y, Zhang Y, Liu Y, Xu J and Chen W 2000 LD pumped Cr^{4+}, Nd^{3+}:YAG with self-*Q*-switched laser output of 1.4 W *Opt. Lett.* **25** 1101–3
[8] Wang P, Zhou S, Lee K K and Chen Y C 1995 Picosecond laser pulse generation in a monolithic self-*Q*-switched solid-state laser *Opt. Commun.* **114** 439–41
[9] Dong J and Ueda K 2006 Observation of repetitively nanosecond pulse-width transverse patterns in microchip self-*Q*-switched laser *Phys. Rev.* A **73** 053824
[10] Dong J, Lu J and Ueda K 2004 Experiments and numerical simulation of a diode-laser-pumped Cr, Nd:YAG self-*Q*-switched laser *J. Opt. Soc. Am.* B **21** 2130–6
[11] Koechner W 1999 *Solid State Laser Engineering* (Berlin: Springer) chapter 5
[12] Dong J, Rapaport A, Bass M, Szipocs F and Ueda K 2005 Temperature-dependent stimulated emission cross section and concentration quenching in highly doped Nd^{3+}:YAG crystals *Phys. Status Solidi* a **202** 2565–73
[13] Rapaport A, Zhao S Z, Xiao G H, Howard A and Bass M 2002 Temperature dependence of the 1.06-μm stimulated emission cross section of neodymium in YAG and in GSGG *Appl. Opt.* **41** 7052–7